Regularities of imaging with gated vision systems

V.V. Belov

Institute of Atmospheric Optics,
Siberian Branch of the Russian Academy of Sciences, Tomsk

Received August 28, 2002

The characteristics of object images observed through scattering media using an active vision system operating with space selection are estimated using the Monte Carlo method. The influence of the optical and geometric conditions of observations on the contrast of images of reflecting objects is considered. The dependences obtained are interpreted.

Introduction

Numerous papers, most of which are generalized, for example, in Refs.1 to 3 are devoted to the study of regularities of imaging and image transfer in vision systems (by vision systems we imply here systems comprising the object's plane, optical device, and scattering medium between them). Most of the papers consider passive vision systems, i.e., the situations when a source of illumination is either absent (a luminous object) or it is external, not being a part of the system (Sun, Moon, stars, etc.).

Among the papers devoted to active vision systems (i.e., those including a pulsed or continuous-wave optical source illuminating an object), to be noted are Refs. 4 and 5. Finally, some problems of imaging in active vision systems with a gated photodetector that implement the so-called spatial selection principle are considered in Refs. 6 and 7. The main advantage of vision systems with spatial selection is well known: they eliminate the background due to backscattered radiation coming from the regions of the medium situated before and after the boundaries of the object space cut out by a time gate.

Despite the fact that a considerable part of the results on vision through turbid media was obtained from experiments and solution of the radiative transfer equation (RTE) by approximate methods, the role of asymptotically exact methods of RTE solution and, in particular, the Monte Carlo method remains significant. This method is used to obtain new information and estimate the applicability limits of the approximate RTE solutions, as well as to check the adequacy of the existing mathematical models to physical processes lying in the basis of imaging and image transfer through scattering and absorbing media. In this paper, the Monte Carlo method is applied for the first time to study the effect of observation conditions on the image quality in a vision system with a gated photodetector.

Statement of the problem and method of solution

Let a pulsed source of radiation be placed at a point S of a Cartesian coordinate system (Fig. 1) and its radiation at the wavelength λ diverges within the angle of $2\nu_0$. The optical axis of the source is oriented along the axis Oy and spaced from it by distance h.

The plane xOy coincides with the homogeneous reflecting surface R characterized by the reflection coefficient α and the coefficient (or diagram) of directional reflection $G(\boldsymbol{\omega})$, where $\boldsymbol{\omega}$ is the unit vector along the direction of propagation of the reflected ray.

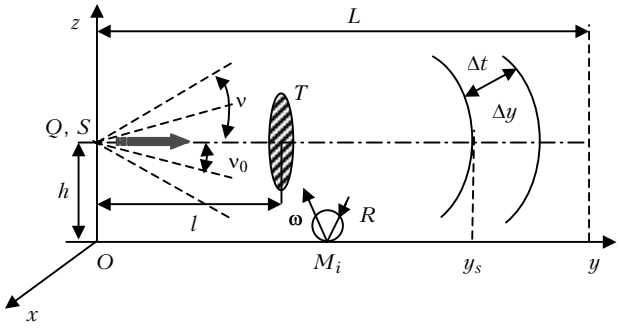

Fig. 1. Geometry of the numerical experiments.

The object T is at the distance l from the source, and the source's optical axis passes through its center. The object is oriented parallel to the plane xOz and is a unit area circle with the radius r_0. Its reflecting properties are characterized by the coefficient ρ and the directional pattern $F(\boldsymbol{\omega})$.

The receiver Q is an ideal optical imaging system and its optical axis coincides with the source's optical axis. The receiver field of view is 2ν. It is assumed that the receiver is opened by a gating pulse to start imaging from the time $t_s = y_s/c$ to the time

$$t_s = (y_s + \Delta y)/c,$$

where c is the speed of light (Δy is called the gate length).

A scattering and absorbing medium fills the space above the surface R (Fig. 1) between the plane xOz and the parallel plane passing through the point $y = L$.

Its optical properties are characterized by the scattering and extinction coefficients ($\beta_{sct}(\mathbf{r}) = \beta_{sct}(y)$, $\beta_{ext}(\mathbf{r}) = \beta_{ext}(y)$, where $\mathbf{r}$ is the radius vector of a point in the medium), the quantum survival probability (single scattering albedo) χ, and the scattering phase

0235-6880/02/11 861-06 $02.00

function $g(\mu)$, where μ is the cosine of the angle θ between the directions of the rays before and after the scattering event. In other words, it is assumed that the medium screening the object from an observer is a monodisperse or polydisperse ensemble of spherical particles, whose concentration can vary along the coordinate y.

Before writing the characteristics of the received radiation needed for estimation of the image quality, let us consider its structure. It is obvious that three elements can be separated out from the image formed by the vision system with continuous illumination (or when $\Delta t > 2L/c$): the image itself, the reflecting surface above which it is located, and the background formed by scattering in the medium. In the gated mode of operation at pulsed illumination, the image may contain from one to three elements depending on the relation between h, l, ν, and y_s.

Thus (see Fig. 2), if (a) $y_s + \Delta y < l$ and $y_s + \Delta y < h\cot(\nu)$, then the object and the surface R are absent in the image; if (b) $y_s > l$ and $y_s > h\cot(\nu)$ (this area is called the shadow zone), then the image consists of two elements (the surface R and the background); if (c) $y_s < l < y_s + \Delta y$ and $y_s > h\cot(\nu)$, then all the three elements are present in the image; and, finally, if (d) $y_s < l < y_s + \Delta y$ and $y_s < h\cot(\nu)$, then the image is formed by the scattered background and the radiation reflected from the object.

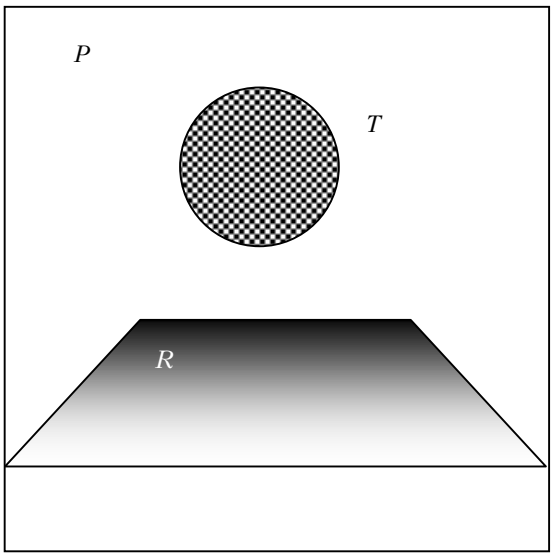

Fig. 2. Image frame

Let our task be to estimate the quality of the image elements. This quality is characterized by the contrast coefficients:

$$k_{TF} = (I_{RT} - I_{RF})/(I_{RT} + I_{RF}), \quad (1)$$

$$k_{TR} = (I_{RT} - I_{RR})/(I_{RT} + I_{RR}), \quad (2)$$

$$k_{RF} = (I_{RR} - I_{RF})/(I_{RR} + I_{RF}), \quad (3)$$

where I_{RF} is the brightness of the background due to scattering (P region in Fig. 2), I_{RT} is the brightness of the object (T), and I_{RR} is the brightness of the reflecting surface (R). The values of the coefficient apparently depend on the coordinates of points on the object, on the reflecting surface, or in the medium (within the space cut out by the gate), i.e., they are functions of two variables (as well as the functions entering into the right-hand side of Eqs. (1)–(3)). Besides, these functions in the general case are functions of time.

Assume that the receiver integrates light fluxes for the time corresponding to the gate length and restricts our consideration to only mean values of the coefficients (1)–(3). That is, I_{RT}, I_{RF}, and I_{RR} will be estimated as mean values in the field of view of the receiving system with a gated photodetector.

To determine their values, one should know the following characteristics of light fluxes generated by the source or recorded by the detector within the gate interval.

1. Object illumination generated by a pulsed source:

$$E_T = E_N + E_{DM} + E_{DR} + E_{NR}, \quad (4)$$

where E_N is the non-scattered radiation from the source; E_{DM} is illumination generated by the diffuse background (scattering of radiation from the source in the medium); E_{NR} is the object illumination by the non-scattered radiation reflected from the surface R (i.e., from the points M_i lying in the receiver's field of view, see Fig. 1); E_{DR} is the diffuse illumination of the object by the radiation reflected from the surface due to scattering in the medium.

2. The intensity of radiation scattered in the medium (but not reflected from the object) in the direction to the receiver:

$$I_{RD} = I_{DM} + I_{DR}, \quad (5)$$

where I_{DM} is the intensity of radiation scattered in the medium, but not reflected from the object; I_{DR} is the intensity of the light flux scattered in the medium after reflection from the surface R, but not reflected from the object.

3. Intensity of the light flux reflected from the object:

$$I_T = F(\omega)E_T. \quad (6)$$

4. Intensity of the background due to scattering (P region in Fig. 2):

$$I_{RF} = I_{RD} + I_{TRD} + I_{TDM}, \quad (7)$$

where I_{TDM} is the intensity of the light flux scattered in this direction after reflection from the object, but not reflected from the surface R; I_{TRD} is the intensity of the radiation scattered in the medium after reflection from the surface R during propagation from the object.

5. Radiation intensity in the object–receiver direction (T region in Fig. 2):

$$I_{RT} = I_{TN} + I_{RF}, \quad (8)$$

where I_{TN} is the intensity of non-scattered radiation reflected by the object.

6. Intensity of radiation recorded by the detector from the surface R:

$$I_{RR} = I_{IRN} + I_{TRN} + I_{RF}, \quad (9)$$

where I_{IRN} is the non-scattered radiation reflected by the surface at its illumination by the source; I_{TRN} is the non-scattered radiation reflected by the surface at its illumination by the object.

Thus, to estimate the quality of the image in the active vision system with a gated photodetector (for the observation geometry shown in Fig. 1) using criteria (1) to (3), it is necessary to find the light fluxes (7) to (9) propagating from the source to the object, scattered or absorbed by the medium, and reflected or absorbed by the surface R and the object T. In addition, the processes of multiple scattering and re-reflection cannot be excluded from consideration if the conditions for their appearance exist. It is just this situation that is considered in this paper.

For statistical estimation of the characteristics (4)–(9), specialized programs were developed that simulate, using the Monte Carlo method, the process of propagation and recording of optical radiation in the system (source S – medium – surface R – object T). The programs are based on the local estimate method[8] and implemented on Turbo Pascal, Version 7.0 (Borland International, Inc.).

Results of numerical experiments

The parameters in Eqs. (4)–(9) have been statistically estimated for the following observation conditions: path length L up to 300 m, optical depth of the medium up to 6 ($\beta_{ext} = 0.02$ m^{-1}), height $h = 1$ m. The angular divergence of the illumination beam is equal to the receiver's field of view and $\nu_0 = \nu = 7°$. The directional patterns $G(\omega)$ and $F(\omega)$ of reflection from the surface R and from the object T correspond to the Lambertian reflection law, and the reflection coefficients satisfy the following conditions: $0 < \alpha$, $\rho \le 1$. The scattering medium is homogeneous in the space $y > 0$ and $z > 0$.

As a generator of characteristics of directed light scattering, we used the software package,[9] with which we selected three forms of the scattering phase function $g(\mu)$ allowing us to simulate the scattering properties of the near-ground urban aerosol, advective fog, and radiative fog at the wavelength $\lambda = 0.86$ μm. The gate length Δy (see Fig. 1) varied from 10 to 40 m.

Computations were performed by the following scheme. At the first stage, E_{DM}, E_N, E_{DR}, I_{RD}, I_{DM} entering into Eqs. (4) and (5) were simulated. Then the components of radiation reflected by the test object and propagating in the direction to the receiver, i.e., I_{IRN}, I_{TRN}, I_{TD}, I_{TDM} in Eqs. (7) and (8), were estimated (using the Monte Carlo method). Finally, after computation of E_N, I_T, I_{TN}, I_{RT}, I_{RF}, and I_{RR}, the contrast coefficients k_{TF}, k_{TR}, and k_{RF} were calculated. Since the effect of the single scattering albedo χ and the reflection coefficients α, ρ on the image quality can be easily predicted, let us analyze the results of numerical experiments connected with the dependence of the characteristics (1)–(3) on the optical depth of the medium τ, the shape of the scattering phase function $g(\mu)$, and the gate length Δy (or gate duration Δt).

The typical dependence of the contrast coefficients k_{TF}, k_{TR}, and k_{RF}, obtained for the case $y_s = l$ (see Fig. 1) using the method of statistical simulation is shown in Fig. 3 for the aerosol model of the medium at $\chi = 0.999$, $\alpha = \rho = 1$, $h = 1$ m, $\tau = L\beta_{ext} = 6$.

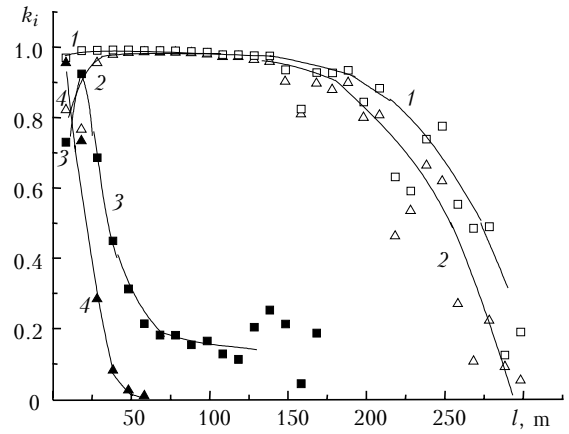

Fig. 3. Dependence of the image contrast coefficients k_i on the distance l.

Numerical experiments, whose results are depicted in Fig. 3, took several hours (Pentium II computer, 433 MHz). If the shape of the scattering phase function is characterized by the coefficients

$$\gamma = \int_0^1 g(\mu)\, d\mu \Big/ \int_{-1}^0 g(\mu)\, d\mu, \quad \xi = \frac{g(1)}{g(-1)}, \quad (10)$$

then for this case they are the following: $\gamma = 0.7995$, $\xi = 1637$.

Let us consider the dependence of the contrast coefficient (1) characterizing the quality of the object vision against the background of the light flux reflected from the medium (against the background of the P region in Fig. 2). From the dependence $k_{TF} = k_{TF}(l)$ obtained for $\Delta y = 10$ m and shown in Fig. 3 as curve *1*, it follows that as the object recedes from the observer to the far boundary of the scattering medium, the image quality for the test object first increases somewhat, then depends only slightly on the distance l, and finally decreases rather rapidly starting roughly from $l > L/2$. The range of variability (at displacement of the gate and the object along the 300-m long path) is $\Delta k \approx 0.1$–0.98.

The dependence $k_{TF} = k_{TF}(l)$ at $l < 40$ m can be explained by the fact that in this case the gate cuts out the space near the source of illumination, where the backscattered radiation is most intense. It should be taken into account that as an object we take the element of a flat surface situated at the far (from the source) boundary of the medium layer cut out by the gate. In this case, the values of the factor characterizing variation of the density of the diverging beam with the distance from the source may differ somewhat for the object (y_s^{-2}) and for the scattering medium at its boundary closest to the source ($(y_s - \Delta y)^{-2}$).

The further increase of y_s smoothes this difference, what can cause insignificant variation of the contrast coefficient as the test object approaches the layer boundary $y_s \to L$ (see Fig. 1). This is also favored by the relative increase (with the increase of y_s) of the reflected radiation formed by photons coming to the receiver at the time corresponding to the distance $y_s + \Delta y$ (see Fig. 1), but from the space preceding to the layer cut out by the gate. This effect is caused by the increase in the photon lifetime due to multiple scattering as considered in detail in Refs. 10 and 11 for roughly the same scheme of numerical experiments.

Variation of the object image contrast with respect to the surface R with the distance from the source is described by the curve *2* in Fig. 3. Note that $k_{TR}(l) < k_{TF}(l)$ in the whole range of the parameter l variability. This can easily be explained by taking into account that the surface is Lambertian and not absorbing. The dependences $k_{TR}(l)$ and $k_{TF}(l)$ are similar, but k_{TR} changes more strongly at y_s (or l) $\to 0$. This is caused by the fact that the factor y_s^{-2} becomes significant in this case (object illumination and the intensity of the flux reflected from the object are proportional to this factor), while for the surface this factor (depending on the position of a point observed on the surface) varies from y_s^{-2} to $(y_s - \Delta y)^{-2}$.

Curve *3* in Fig. 3 characterizes the dependence of the contrast coefficient k_{RF} for the image of the surface R against the scattered background (P region in Fig. 2) on the distance l between the source of illumination and the object. This dependence differs markedly from those considered above by the fact that it peaks at a far smaller l and $k_{RF} < 0.1$ already at $l \approx 100$ m (while k_{TR} and $k_{TF} > 0.8$ in this range of l values). This result is obvious, and to explain it, it is sufficient to compare the curves $k_{TR}(l)$ and $k_{TF}(l)$ in Fig. 3.

Let us note the general feature of $k_i(l)$ estimates obtained in numerical experiments. With the increase of l, as the object approaches the far boundary of the medium, the accuracy of the estimates of light flux characteristics used for calculating k_i decreases. Statistical outliers are especially intense when simulating reflected fluxes. They also appear when calculating k_i at $l \to L$. The cause for appearance of these outliers and some methods to eliminate them are known and described in Ref. 3.

Consider now the dependence of the quality of imaging the objects observed through a scattering screen on the gate length. Figure 4 depicts the estimates of the contrast coefficients $k_{TF}(l)$ for the aerosol model of the screen and different gate lengths Δy. These estimates show that the dependence of the object contrast against the background (P region in Fig. 2) $k_{TF}(l)$ transforms, as the gate length grows, in the following way. The image contrast decreases, and the closer the object is to the medium boundary, the stronger is this decrease. However, the causes of this dependence $k_{TF}(l)$ at the two intervals of l variation are different.

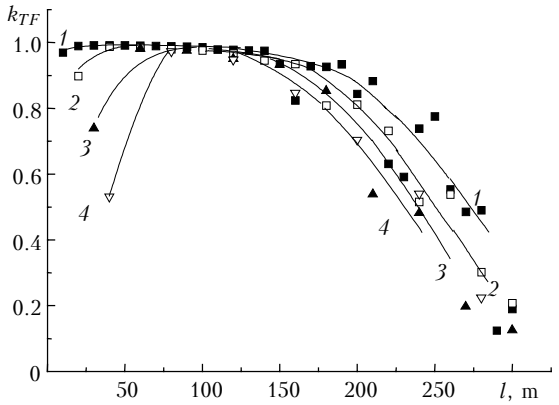

Fig. 4. Effect of gate length on the object-to-background contrast of an image: 10 (*1*), 20 (*2*), 30 (*3*), 40 m (*4*).

At $l \to 0$ the cause of the contrast decrease is as described above being connected with the dependence of the intensity of diverging beams on the geometric factor equal to $(r \approx \Delta y/2)^{-2}$ for the scattering medium and Δy^{-2} for the object. The growth of the gate length strengthens the effect of this factor on the signal intensity and scattering background.

At $l \to L$, as was already mentioned, the effect of this factor decreases, but simultaneously the illumination of the object decreases and the contribution of multiply scattered radiation from the medium region $y < y_s$ to the scattering background increases. Gate elongation leads to an increase of the effect of these factors on I_{RF} and I_{RT}, thus leading to a relative decrease of I_{RT} and increase of I_{RF}, making their values closer.

As the gate length changes, even more significant changes occur in the dependence of the quality of the surface R image (in terms of the contrast coefficient k_{RF}) against the background of the diffusely luminous medium. These are illustrated in Fig. 5, which depicts the dependence $k_{RF} = k_{RF}(l)$ for the same values of Δy as in Fig. 4. Pulse gate elongation leads to broadening of the function $k_{RF}(l)$ and shift of its peak toward the far (from the source) boundary of the medium. As this takes place, the contrast of the image of far (from the observer) area of the surface R increases. Thus, for example, the value of $k_{RF}(120)$ increases almost threefold.

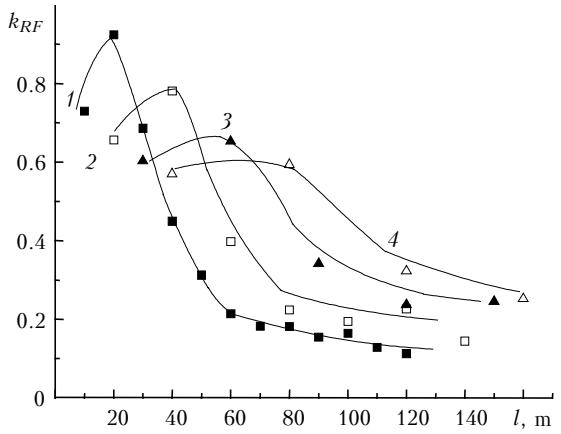

Fig. 5. Effect of the gate length on the surface-to-background contrast of the image: 10 (*1*), 20 (*2*), 30 (*3*), 40 m (*4*).

To explain these changes, one should take into account that as l and the gate length increase, the area of the surface image increases [in contrast to the test object, whose *visible* area depends only on l (decreases with the increasing l) and does not depend on the gate length]. At the same time, the increase of the gate length leads to an increase of the flux of scattered radiation coming from the P region to the receiver. This growth turns out to prevail over the growth of the signal at the initial part of the path ($l \to 0$).

The effect of scattering properties of the medium and, in particular, the shape of the scattering phase function on the light fluxes taking part in imaging is illustrated in Fig. 6. This figure shows the characteristic $\eta = I_n/(I_n + I_{nd})$, where I_n is the non-scattered radiation reflected from the object neglecting object illumination by the radiation scattered in the medium and $I_n + I_{nd}$ is the same but with the allowance for illumination by scattered radiation.

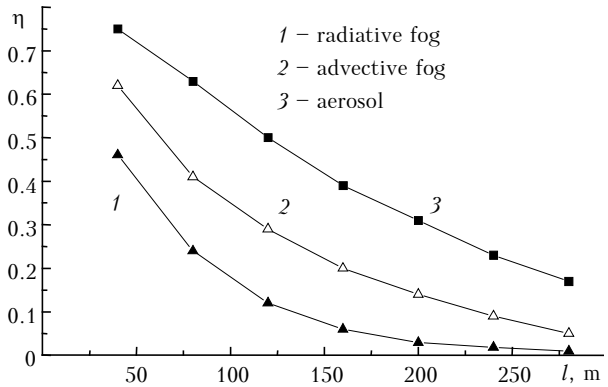

Fig. 6. Effect of diffuse illumination on the intensity of non-scattered radiation reflected from the object.

We can see that as the forward peak of the scattering phase function increases, the effect of diffuse illumination of the object on the intensity of the light flux reflected from the object increases markedly. The contribution of the diffuse illumination to the total object illumination increases monotonically with increasing l. This is caused by the fact that the scattering process in media with a smaller forward peak of the scattering phase function leads to a more rapid broadening of the illumination beams and, consequently, to the decrease of the intensity of scattered radiation while keeping its initial direction of propagation. When interpreting the dependences shown in Fig. 6, we should also take into account that with the increase of $l > r_0 \cot(\nu_0)$ the non-scattered radiation incident on the object decreases proportionally to $\pi\, l^{-2} \cot^2(\nu_0)$.

In these numerical experiments, the relative characteristics of the forward peak of the scattering phase function took the values $\gamma = 0.7995$, $\xi = 1637$ (aerosol), $\gamma = 0.945$, $\xi = 723$ (advective fog), and $\gamma = 0.989$, $\xi = 27200$ (radiative fog).[9]

Conclusions

The main results obtained in this work are the following:

1. A software package of the Monte Carlo method has been developed for statistical simulation of the imaging process in pulsed active vision systems with spatial selection. It accounts for the effect of multiple scattering in the medium and reflection (re-reflection) from the surface at propagation of the illuminating pulse to the object and radiation reflected from the object. These computer codes can be applied to analysis of the image quality in optoelectronic navigation systems with spatial selection.

2. In the framework of the problem formulated, the contrast of the object image against the scattered background and the surface lying under the observation path exceeds the level of 0.8 up to the optical depth of the medium $\tau \approx 4$ and exceeds 0.4 up to $\tau \approx 5$. The limiting optical depth, at which the contrast coefficient is still higher than 0.05, lies in the interval $\tau \approx 5$–6. The contrast of the surface image against the background of radiation scattered in the medium decreases rapidly with the increasing distance from the object to the receiver and remains at the level of 0.05 at $\tau \approx 1$–2.

3. The process of multiple scattering determines, to a significant degree, not only the backscattering, but also the signal and, in particular, the intensity of non-scattered radiation reflected by the object and recorded with the detector (see Fig. 6).

Application of the method of spatial selection in pulsed active vision systems leads to a significant increase of the image contrast of an object screened from the observer by a layer of a dense scattering medium. This can lead to the almost tenfold increase of the visibility range at the same level of the image contrast (curve *4* corresponding to the mode without spatial selection and curve *1* in Fig. 3).

Acknowledgments

The author is thankful to Dr. B.D. Borisov for useful discussions on the results of statistical experiments considered in this paper.

References

1. E.P. Zege, A.P. Ivanov, and I.L. Katsev, *Image Transfer in Scattering Medium* (Nauka i Tekhnika, Minsk, 1985), 327 pp.
2. T.A. Sushkevich, S.A. Strelkov, and A.A. Ioltukhovskii, *Method of Characteristics in Problems of Atmospheric Optics* (Nauka, Moscow, 1990), 296 pp.
3. V.E. Zuev, V.V. Belov, and V.V. Veretennikov, *Theory of Systems in Optics of Disperse Media* (Spektr, Tomsk, 1997), 402 pp.
4. D.M. Bravo-Zhivotovskii, A.G. Luchinin, and V.A. Savel'ev, Izv. Akad. Nauk SSSR, Ser. Fiz. Atmos. Okeana **5**, No. 7, 672–684 (1969).
5. M.P. Vanyukov, E.V. Nilov, and A.A. Chetkov, Opt.-Mekhan. Promyshlennost, No. 6, 50–55 (1970).
6. I.L. Katsev, E.P. Zege, and A.S. Prikhach, in: *Proceedings of III Inter-Republic Symposium on Atmospheric and Ocean Optics* (Tomsk, 1996), p. 158.
7. V.G. Volkov, Tekhnika Kino i Televideniya, No. 5, 31–34 (2001)
8. G.I. Marchuk, ed., *Monte Carlo Method in Atmospheric Optics* (Nauka, Novosibirsk, 1976), 216 pp.
9. F.X. Kneizys, G.P. Anderson, E.P. Shettle, W.O. Gallery, L.W. Abreu, J.E. Selby, J.H. Chetwynd, and S.A. Clough, *User Guide to LOWTRAN 7*, Hanscom AFB, MA01731: AFGL–TR–86–01777. ERP. No. 1010 (1988).
10. V.V. Belov and A.B. Serebrennikov, Atmos. Oceanic Opt. **13**, No. 8, 671–676 (2000).
11. V.V. Belov and A.B. Serebrennikov, Atmos. Oceanic Opt. **14**, No. 3, 222–224 (2001).